Common laboratory mice are susceptible to infection with SARS-CoV2 beta variant

Ravi Kant (Ravi.kant@helsinki.fi)
University of Helsinki https://orcid.org/0000-0003-3878-9775

Lauri Kareinen
University of Helsinki

Teemu Smura
University of Helsinki

Tobias L. Freitag
University of Helsinki

Sawan Kumar Jha
University of Helsinki

Kari Alitalo
University of Helsinki

Seppo Meri
University of Helsinki

Tarja Sironen
University of Helsinki

Kalle Saksela
University of Helsinki

Tomas Strandin
University of Helsinki

Anja Kipar
University of Zurich

Olli Vapalahti
University of Helsinki

Short Report

Keywords: SARS-CoV-2, COVID-19, VOCs, SARS-CoV-2 Variants

Posted Date: July 30th, 2021

DOI: https://doi.org/10.21203/rs.3.rs-762916/v1

Version of Record: A version of this preprint was published at Viruses on November 11th, 2021. See the published version at https://doi.org/10.3390/v13112263.

Abstract

Small animal models are of crucial importance for assessing COVID-19 countermeasures. Common laboratory mice would be well-suited for this purpose but are not susceptible to infection with wild-type SARS-CoV-2. Herein we show that the SARS-CoV-2 beta variant attains infectibility to BALB/c mice and causes pulmonary changes consistent with COVID-19.

Background

The COVID-19 pandemic has devastated the world since the emergence of SARS-CoV-2 in late 2019. The pathogenesis of COVID-19 includes an acute pneumonia that can develop into an acquired respiratory distress syndrome (ARDS) (1-3). The effective spread of SARS-CoV-2 among the human population is potentiated by the emergence of highly transmittable variants of concern (VOCs) some of which can evade previously acquired immunity and cause more severe disease than the “wild-type” (wt) strains originating from Wuhan, the D614G mutant of which was dominating the pandemic until the end of 2020. As declared by the World Health Organization (WHO), the nomenclature of currently circulating VOCs are alpha (B.1.1.7 by Pango nomenclature), beta (B.1.351), gamma (P.1) and delta (B.1.617.2) (4).

The rapid development of vaccines and studies of antiviral drugs against SARS-CoV-2 are of prime importance and have been made possible by animal models that recapitulate human SARS-CoV-2 infection and the associated disease. Several animal species, such as Syrian hamsters and non-human primates, have been documented as suitable platforms to experiment *in vivo* with various COVID-19 countermeasures (5). In contrast, common laboratory mice have proven refractory to infection due to mouse-specific differences in the SARS-CoV-2 entry receptor, the Angiotensin Converting Enzyme (ACE)-2 (1). However, using mice as the model species would provide unrivaled benefits over any other animal species by facilitating the use of an army of tools to study host genetics and immune responses developed for decades by the scientific community. Introduction of human ACE-2 (hACE-2) into mice partially overcomes this drawback but this model is less widely available and requires laborious and expensive breeding to make use of the numerous existing gene modified mouse strains. Also, hACE-2 “knock-in” mouse models are not adequate for all questions, as they do not faithfully mimic the natural expression pattern of the ACE-2 receptor (5).

Instead of mutating the host, SARS-CoV-2 infection models in mice have also been achieved by mutating the virus either by reverse genetics or by serial passaging through mouse lungs (6-9). By these means a few key residues that improve the affinity of the SARS-CoV-2 spike S1 protein to mouse ACE-2 (mACE-2) and increased infectivity of SARS-CoV-2 in standard BALB/c mice have been observed (7, 8). Interestingly, some of these mutations appear also in circulating VOCs, such as the N501Y mutation present in alpha, beta and gamma. This suggests that clinical VOC isolates possess improved infectivity over wt SARS-

CoV-2 in mice. In order to test this hypothesis, we compared the infectivity and pathological effects of a clinically isolated beta variant to wt SARS-CoV-2 in the lungs of BALB/c mice after intranasal inoculation.

The Study

We intranasally inoculated 9 to 12 week old female BALB/c mice with 2 x 10^5 plaque-forming units (PFU) of wt and beta SARS-CoV-2 (9), and assessed virus replication, viral antigen expression and associated pathological changes in the lungs at 2 and 3 days post infection (dpi) by analyzing the viral RNA loads by RT-qPCR and antigen expression by immunohistochemistry (IHC). We detected high amounts of SARS-CoV-2 RNA in mice infected with the beta variant as indicated by low Ct values in RT-qPCR (Fig. 1) for the RNA dependent RNA polymerase (RdRp) and envelope (E) genes as well as the subgenomic E gene (subE; replication-intermediate (10)). None of the viral RNA targets were detectable in the lungs of mice infected with wt/D614G SARS-CoV-2, as shown previously (11).

Successful replication of beta SARS-CoV-2 in BALB/c mice was evident also by IHC which consistently detected virus antigen in intact and partly degenerate bronchial/bronchiolar epithelial cells and a few tracheal epithelial cells at 2 dpi (Fig. 2A-B). Scattered alveoli exhibited viral antigen in type I and II pneumocytes (Fig. 2C-D); some activated type II pneumocytes and occasional degenerate of type I pneumocytes were observed. Abundant viral antigen was often covering the luminal surface of bronchiolar epithelial cells. Bronchioles with more extensive viral antigen expression and degeneration of bronchial epithelial cells exhibited leukocyte infiltration of the wall and viral antigen within infiltrating macrophages. Adjacent arteries showed endothelial cell activation. At 3 dpi, alveolar viral antigen expression was more widespread and associated with clear evidence of alveolar damage. Focally, alveoli contained vacuolated macrophages, erythrocytes and degenerate/necrotic epithelial cells (Fig. 2F-H), consistent with focal necrotic pneumonia. In these areas, the vascular response was more intense, with endothelial cell activation and occasional rolling and emigration of leukocytes. The observed changes are morphologically similar to those observed in K18-hACE2 mice at 3 dpi with a wt strain, though less extensive (12). Bronchial lymph nodes generally exhibited SARS-CoV-2 antigen in several macrophages and/or dendritic cells (Fig.2I). In contrast, mice infected with wt SARS-CoV-2 did not show any histological changes and no viral antigen expression at 2 and 3 dpi (data not shown).

We also attempted intranasal inoculations with lower doses (6 x 10^4 and 6 x 10^3 PFU) and examined the animals at 2 dpi. In all mice the infection established in the nose, with viral antigen expression in patches of respiratory and olfactory epithelial cells (Supplemental Fig. S1A). This was occasionally associated with leukocyte recruitment (rolling) in vessels beneath the infected epithelium, consistent with an early inflammatory response. In most animals the virus had apparently not reached the lung, as IHC and PCR gave inconsistent and partly discordant results, probably because each one half of the lungs was processed for either methodological approach. However, the detection of viral antigen in tracheal, bronchiolar and, rarely, alveolar epithelial cells confirmed that infection could be achieved. Even at 4 dpi, the lungs were not consistently infected. When we co-housed 3 naïve mice with one intranasally (6 x 10^4 PFU) infected mouse (n =3), no evidence of infection in the co-housed animals were observed after 4 dpi

as confirmed by IHC on nose and lungs, suggesting that viral shedding from the nose was insufficient for transmission to the naïve mice. These results suggest that optimal dosing of beta variant is in the 10^5 PFU range to consistently achieve infection of the lungs, at least when applied through the intranasal route. No new viral mutations were detected in the lungs of infected mice as compared to the inoculated SARS-CoV-2 beta variant (data not shown).

Conclusions

The wt SARS-CoV-2 is unable to infect mice due to a receptor mismatch, but accumulating evidence suggests that naturally occurring VOCs might be able to acquire this function (5, 13). We probed this hypothesis and show that BALB/c mice are susceptible to infection with the beta variant producing a mild pneumonia reminiscent of what is seen in the K18-hACE2 mice and other species susceptible to SARS-CoV-2 (12). Further studies are needed to determine which other variants are similarly able to infect laboratory mice, the genetic determinants required and whether the acquired ability to infect mice is related to an increased affinity towards mACE-2 specifically or to ACE-2 across species (including hACE-2); the latter is likely given the evidently increased transmissibility of VOCs in humans (4, 13).

Our findings indicate options to experimentally approach various COVID-19 countermeasures in an unprecedented scale, since the standard laboratory mouse has several advantages over other animal models used in infectious disease experimentation, including cost-effectiveness, ease of handling, and suitability for large-scale studies.

Declarations

Acknowledgements

We thank Sanna Mäki and Johanna Martikainen and the laboratory technicians of the Histology Laboratory, Institute of Veterinary Pathology, Vetsuisse Faculty, University of Zurich, for expert technical assistance. This research is funded by the Academy of Finland iCOIN (grant number 336490).

The authors declare no competing interests.

References

1. Zhou P, Yang XL, Wang XG, Hu B, Zhang L, Zhang W, et al. A pneumonia outbreak associated with a new coronavirus of probable bat origin. Nature. 2020;579(7798):270-3.

2. Zhu N, Zhang D, Wang W, Li X, Yang B, Song J, et al. A Novel Coronavirus from Patients with Pneumonia in China, 2019. N Engl J Med. 2020;382(8):727-33.

3. Xu Z, Shi L, Wang Y, Zhang J, Huang L, Zhang C, et al. Pathological findings of COVID-19 associated with acute respiratory distress syndrome. Lancet Respir Med. 2020;8(4):420-2.

4. Konings F, Perkins MD, Kuhn JH, Pallen MJ, Alm EJ, Archer BN, et al. SARS-CoV-2 Variants of Interest and Concern naming scheme conducive for global discourse. Nat Microbiol. 2021;6(7):821-3.

5. Renn M, Bartok E, Zillinger T, Hartmann G, Behrendt R. Animal models of SARS-CoV-2 and COVID-19 for the development of prophylactic and therapeutic interventions. Pharmacol Ther. 2021;228:107931.

6. Dinnon KH, 3rd, Leist SR, Schäfer A, Edwards CE, Martinez DR, Montgomery SA, et al. A mouse-adapted model of SARS-CoV-2 to test COVID-19 countermeasures. Nature. 2020;586(7830):560-6.

7. Gu H, Chen Q, Yang G, He L, Fan H, Deng YQ, et al. Adaptation of SARS-CoV-2 in BALB/c mice for testing vaccine efficacy. Science. 2020;369(6511):1603-7.

8. Roy Wong LY, Zheng J, Wilhelmsen K, Li K, Ortiz ME, Schnicker NJ, et al. Eicosanoid signaling as a therapeutic target in middle-aged mice with severe COVID-19. bioRxiv. 2021.

9. Zhang Y, Huang K, Wang T, Deng F, Gong W, Hui X, et al. SARS-CoV-2 rapidly adapts in aged BALB/c mice and induces typical pneumonia. J Virol. 2021;95(11).

10. Dagotto G, Mercado NB, Martinez DR, Hou YJ, Nkolola JP, Carnahan RH, et al. Comparison of Subgenomic and Total RNA in SARS-CoV-2 Challenged Rhesus Macaques. J Virol. 2021;95(8).

11. Bao L, Deng W, Huang B, Gao H, Liu J, Ren L, et al. The pathogenicity of SARS-CoV-2 in hACE2 transgenic mice. Nature. 2020;583(7818):830-3.

12. Clark JJ, Penrice-Randal R, Sharma P, Kipar A, Dong X, Pennington SH, et al. Sequential infection with influenza A virus followed by severe acute respiratory syndrome coronavirus 2 (SARS-CoV-2) leads to more severe disease and encephalitis in a mouse model of COVID-19. bioRxiv. 2021:2020.10.13.334532.

13. Harvey WT, Carabelli AM, Jackson B, Gupta RK, Thomson EC, Harrison EM, et al. SARS-CoV-2 variants, spike mutations and immune escape. Nat Rev Microbiol. 2021;19(7):409-24.

Figures

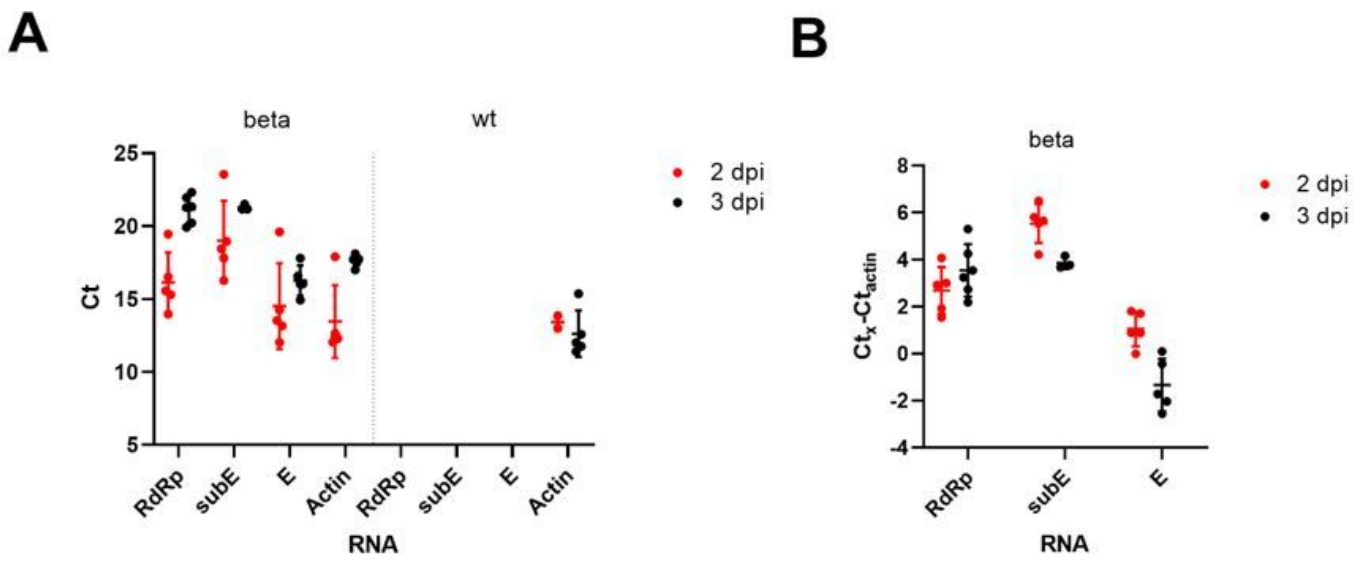

Figure 1

BALB/c mice are susceptible to infection by the beta variant of SARS-CoV-2. 9 to 12-week old female BALB/c mice were intranasally inoculated with 2 x 105 PFU of the beta variant or wt SARS-CoV-2 followed by RT-qPCR analysis of RNA isolated from lungs of infected animals at 2 or 3 days post inoculation (n = 6 or 5 for beta, 2 or 5 for wt, resepctively). (A) The Ct values for genomic RdRp and E genes as well as subgenomic E gene (subE) are shown for both beta and wt infections. Actin mRNA levels served as an internal control target. (B) The normalized Ct values for RdRp, E and subE at 2 and 3 days post inoculation with beta variant. Normalization was achieved by subtracting actin mRNA Ct values from target Cts. Mean ± standard deviation are indicated.

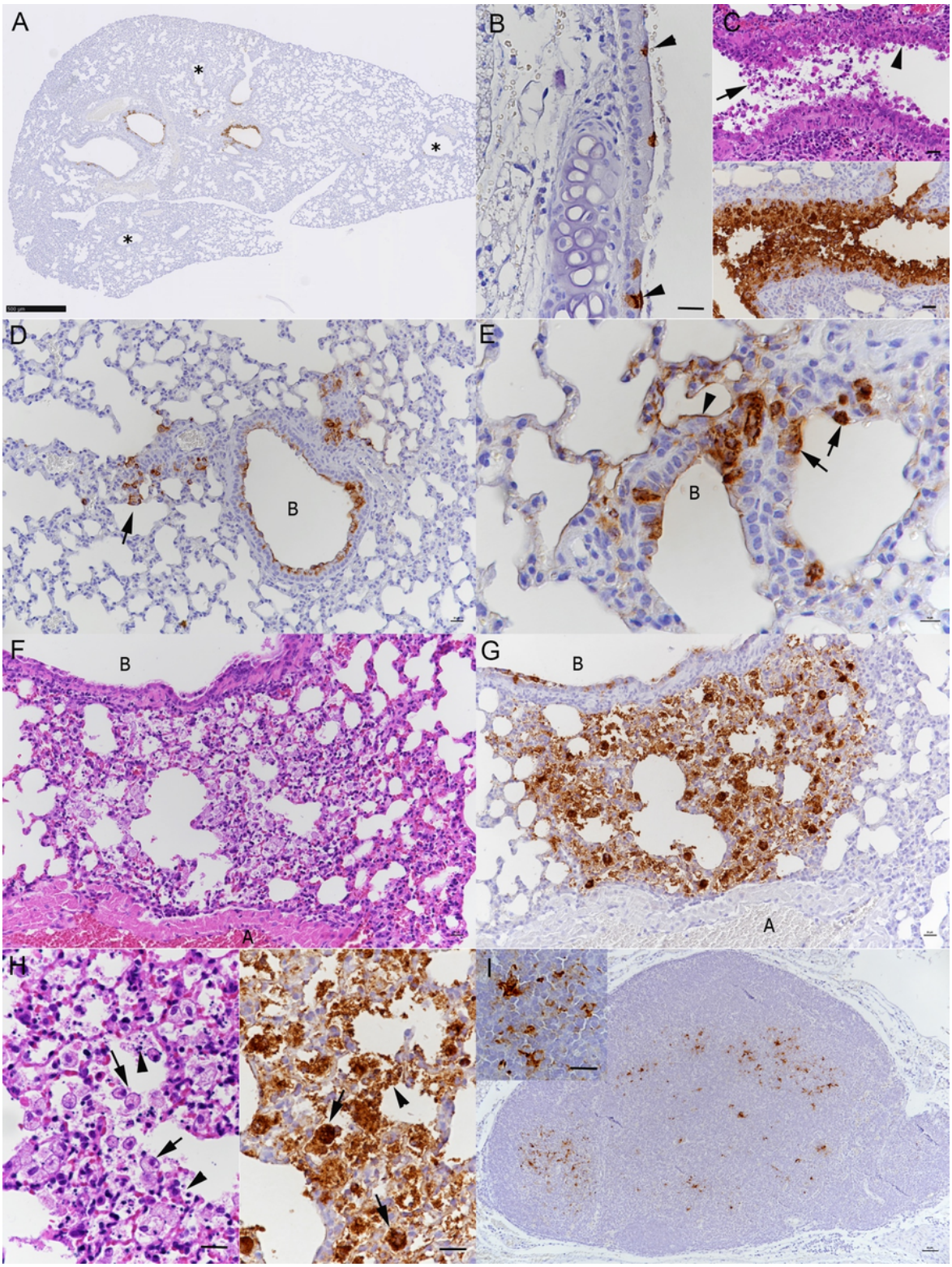

Figure 2

Histopathological assessment and SARS-CoV-2 NP expression of female BALB-C mice after intranasal infection with 2 x 105 PFU of beta variant. A-E. Animal euthanized at 2 days post infection. A. Left lung lobe, longitudinal section, overview. Viral antigen expression in individual to almost all epithelial cells in several bronchioles. Other bronchioles are entirely negative (*). Bar = 500 µm. B. Trachea with a few individual ciliated epithelial cells expressing viral antigen (arrowheads). Bar = 10 µm. C. Lung; larger

bronchiole with degeneration of epithelial cells (arrowhead) and degenerate cells in the lumen (arrow) and extensive viral antigen expression. There is also a mild peribronchiolar lymphocyte infiltration. Bar = 20 µm. D. Lung with viral antigen expression in bronchiolar epithelial cells and pneumocytes in adjacent alveoli (arrow). B: bronchiole. Bar = 20 µm. E. Bronchioalveolar transition. Viral antigen expression is seen in bronchiolar (B) epithelial cells, type I (arrowhead) and type II (arrows) pneumocytes. Bar = 10 µm. F-I. Animal euthanized at 3 days post infection. F, G. Lung with focal area of alveolar damage and accumulation of cells in alveolar lumina, with intense viral antigen expression. A: artery; B: bronchiole. Bars = 20 µm. H. Closer view of the area in F and G, showing degeneration of alveolar epithelial cells (arrowheads) and accumulation of macrophages with cytoplasmic vaculoation and phagocytosed cell debris (arrows), associated with strong viral antigen expression. Bar = 10 µm. I. Bronchial lymph node with viral antigen expression in cells with the morphology of macrophages and dendritic cells (inset). Bar = 20 µm (inset: 10 µm). Hematoxylin stain and immunohistochemistry, hematoxylin counterstain.

Supplementary Files

This is a list of supplementary files associated with this preprint. Click to download.

- SupplementalFigure1.jpg
- AppendixMethodologyReferencesandSuppFig.docx